Point defects in NiAl: The effect of lattice vibrations

A. Y. Lozovoi
Atomistic Simulation Group, School of Mathematics and Physics, Queen's University, Belfast BT7 1NN, United Kingdom

Y. Mishin
School of Computational Sciences, George Mason University, Fairfax, Virginia 22030, USA

(Received 7 May 2003; revised manuscript received 23 July 2003; published 26 November 2003)

We investigate the effect of atomic vibrations on point defect free energies and equilibrium concentrations in the B2 NiAl compound using the quasiharmonic approximation in combination with a recently developed embedded-atom potential. The entropy term appears to be the dominant contribution to the Gibbs free energies of point defects. Vibrational entropies of the main defect complexes: triple-Ni defect, exchange defect, divacancy, and even of the interbranch-Al defect turn out to be positive in the whole range of temperatures studied here (0–1700 K). This leads to an increase in the concentrations of all four types of point defects in Ni-rich and stoichiometric NiAl. On the Al-rich side, the effect of lattice vibrations is to shift the minimum on the vacancy concentration versus temperature curve towards lower temperatures. The effect of zero-point vibrations is shown to be too small to affect the type of constitutional defects in NiAl. The constitutional defects remain nickel antisite atoms on the Ni-rich side and nickel vacancies on the Al-rich side.

DOI: 10.1103/PhysRevB.68.184113 PACS number(s): 61.50.Ah, 73.30.+y, 61.72.Bb, 61.72.Ji

I. INTRODUCTION

The intermetallic compound NiAl demonstrates a number of attractive properties that motivate its extensive use in industry.[1] An equally important role of NiAl is to serve as a model system to investigate basic properties of ordered intermetallic compounds. NiAl is famous for a peculiar atomic mechanism of compositional disorder, which was discovered experimentally by Bradley and Taylor.[2] Namely, deviations from the stoichiometry on the Al-rich side are accommodated by so-called structural vacancies on the Ni sublattice. In contrast, on the Ni-rich side the excess Ni atoms reside on the Al sublattice as antisites. This mechanism of disorder has been supported by several *ab initio* calculations,[3–6] but has recently been questioned based on new experimental data.[7,8] This apparent controversy between theory and experiment continues to be the subject of debate in the literature.[9–11] Another source of concern is the existing discrepancy between measured[12–15] and calculated[3–5] vacancy formation energies in NiAl, the measured values being appreciably lower.[15]

One aspect that has not yet been examined in detail is the possible effect of lattice vibrations on point defects and compositional disorder in NiAl. A study of this effect is the goal of the present paper. We chose to model the atomic vibrations within the harmonic approximation.[16] There are other, arguably more accurate methods of calculating the effect of temperature on thermodynamic properties of solids.[17] Such methods, however, are based on Monte Carlo (MC) or molecular-dynamics simulations and are computationally much more expensive than harmonic calculations. In addition, those methods are based on classical dynamics and, therefore, give no access to quantum effects that can be important at low temperatures. A drawback of the harmonic method is the underestimation of the anharmonicity of atomic vibrations at high temperatures.[17] Recognizing this fact, we believe that our results are accurate at relatively low temperatures but can only be considered as trends at high temperatures. Some of our results are compared with those of independent MC simulations, which were also performed in this work.

Since even harmonic calculations are computationally demanding and their combination with *ab initio* methods is still problematic, using a semiempirical potential offers a more practical approach to the problem. In this work we model atomic interactions in NiAl by an embedded-atom method (EAM) potential constructed in Ref. 18. The potential was fit to both experimental and *ab initio* data for the Ni-Al system and was shown to reproduce various phonon and point defect properties of NiAl in good agreement with experiment and first-principles calculations.[18,19] We therefore expect it to represent the NiAl compound with an accuracy sufficient for the purposes of the present study.

II. BACKGROUND THEORY

A. Harmonic approximation

Consider a simulation block (supercell) of N atoms with a volume V at a temperature T with periodicity imposed in all three dimensions. It is straightforward within the EAM scheme to construct and then diagonalize the dynamical matrix of the block,

$$D_{ij}=\frac{1}{\sqrt{m_i m_j}}\left(\frac{\partial^2 U}{\partial \mathbf{q}_i \partial \mathbf{q}_j}\right),$$

where m_i and $\mathbf{q}_i$ are the mass and coordinates of atom i, and U is the potential energy of the block. This results in $3N-3$ nonzero frequencies ν_α of normal vibrational modes of the supercell. The Helmholtz free energy of the block can be written as a sum of the potential energy U due to static interactions between the atoms, the configurational entropy

term $-TS^{conf}$ due to permutations of unlike atoms and/or vacancies in the crystal, and the free energy due to atomic vibrations (F^{vib}):

$$F(N,V,T)=U(N,V)-TS^{conf}(N,T)+F^{vib}(N,V,T). \tag{1}$$

The vibrational free energy is given by the expression

$$F^{vib}(N,V,T)=k_BT\sum_{\alpha=1}^{3N-3}\ln\left[2\sinh\left(\frac{h\nu_\alpha}{2k_BT}\right)\right], \tag{2}$$

where h and k_B are Planck's and Boltzmann's constants, respectively. If thermal expansion is ignored, the frequencies ν_α are evaluated at the equilibrium volume of the statically relaxed supercell and Eq. (2) represents the so-called *harmonic approximation* (HA). A way to include the thermal expansion is to make the frequencies volume dependent. The equilibrium volume $V(T)$ is then determined by minimizing the total free energy $F(N,V,T)$ with respect to volume under the condition $p=0$ (in the present study we only consider the zero-pressure case). This approach is referred to as the *quasiharmonic approximation* (QHA). We shall keep to this terminology throughout the paper.

The vibrational free energy F^{vib} can be further decomposed as

$$F^{vib}=E^{vib}-TS^{vib},$$

where E^{vib} and S^{vib} are the energy and entropy associated with atomic vibrations:

$$S^{vib}=-\left(\frac{\partial F^{vib}}{\partial T}\right)_V=k_B\sum_{\alpha=1}^{3N-3}\left(\frac{h\nu_\alpha}{k_BT}\right)\frac{\exp(-h\nu_\alpha/k_BT)}{1-\exp(-h\nu_\alpha/k_BT)}-\ln\left[1-\exp\left(-\frac{h\nu_\alpha}{k_BT}\right)\right], \tag{3}$$

$$E^{vib}=F^{vib}+TS^{vib}=\frac{1}{2}\sum_{\alpha=1}^{3N-3}h\nu_\alpha+\sum_{\alpha=1}^{3N-3}h\nu_\alpha\frac{\exp(-h\nu_\alpha/k_BT)}{1-\exp(-h\nu_\alpha/k_BT)}. \tag{4}$$

The first, temperature-independent term in Eq. (4) describes the effect of zero-point vibrations.

Equations (2)–(4) represent the general quantum case. In the classical limit (all $h\nu_\alpha \ll k_BT$), E^{vib} reduces to $(3N-3)k_BT$ and the effect of zero-point vibrations vanishes. Unless otherwise stated, all our calculations are based on the quantum expressions (2)–(4).

B. Free energies of point defects

The statistical-mechanical theory of point defects in ordered compounds[4,5,20–23] is based on the Wagner-Schottky model of a lattice gas of noninteracting point defects.[24] In that model, the energy of a partially ordered crystal is a linear function of the numbers of individual point defects. The equilibrium concentrations of the defects can be found by minimizing the free energy of the crystal with respect to such concentrations subject to certain constraints. The minimization leads to a set of equations of the mass action law type containing point defect energies u_P as input parameters, where P enumerates the types of point defect. It has been shown that atomic vibrations can be incorporated in this formalism by simply replacing the defect energies u_P by their free energies g_P:[22]

$$g_P=u_P+\varepsilon_P^{vib}-Ts_P^{vib}. \tag{5}$$

In this work, the potential energies of individual point defects are treated as their ''raw'' energies[21] defined as the potential energy of a supercell containing $N-1$ regular atoms and one point defect minus the potential energy of a perfect block containing N atoms. The raw vibrational energies ε_P^{vib} and entropies s_p^{vib} are defined by the same scheme.

The B2 crystal structure of NiAl contains two sublattices and supports four types of point defects—vacancies V_{Ni} and V_{Al} and two types of the antisite defects: $\mathrm{Al_{Ni}}$ and $\mathrm{Ni_{Al}}$ (the subscript denotes the sublattice). In the canonical treatment of the problem, the defect concentrations are subject to the constraint of preserving the chosen composition x of the $\mathrm{Ni}_x\mathrm{Al}_{1-x}$ alloy. This constraint reduces the number of degrees of freedom to 3. Hence, only three of the mass action equations are independent. Those three equations are solved numerically for the defect concentrations for a particular temperature T and alloy composition x.

C. Composition conserving defect complexes

The defect raw free energies g_P enter the mass action equations in certain combinations corresponding to quasichemical defect reactions. Such combinations preserve the number of atoms of each species and thus the alloy composition. Combinations of point defects that do not alter the composition of the compound are called *composition conserving defect complexes*, or simply complex defects (cd's).[5,20,22] Examples of cd's in NiAl are a divacancy (Dv) $V_{\mathrm{Al}}+V_{\mathrm{Ni}}$, an exchange defect (Ex) $\mathrm{Ni_{Al}}+\mathrm{Al_{Ni}}$, a triple-Ni defect (TN) $2V_{\mathrm{Ni}}+\mathrm{Ni_{Al}}$, and a triple-Al defect (TA) $2V_{\mathrm{Al}}+\mathrm{Al_{Ni}}$. One can think of cd's as elementary thermal excitations that automatically preserve the alloy composition. The knowledge of the free energies of any three independent cd's completely defines the equilibrium concentrations of all thermal point defects as well as the type of structural defects in the alloy of a given composition. To determine the type of structural defects, one should examine the energies (*not* free energies) of so-called interbranch defects[5] that convert one type of defect to another within the same sublattice. In NiAl, one should consider the interbranch-Al (IA) defect, which creates an Al antisite instead of two vacancies on the Ni sublattice ($-2V_{\mathrm{Ni}}+\mathrm{Al_{Ni}}$), and the interbranch-Ni defect (IN), which does the opposite on the Al sublattice ($-\mathrm{Ni_{Al}}+2V_{\mathrm{Al}}$). For V_{Ni} and $\mathrm{Ni_{Al}}$ to be structural defects in Al-rich and Ni-rich compositions, respectively, the energies of the IA and IN defects must be both positive. This explains why these energies are also referred to as the stability criteria.[22] Interbranch defects can also be viewed as normal thermal excitations in the respective off-stoichiometric alloys. The IA

TABLE I. Relation between the free energies of composition-conserving defect complexes g_{cd} and raw free energies of individual point defects g_P ($P=\mathrm{Ni_{Al}}$, $\mathrm{Al_{Ni}}$, V_{Ni}, and V_{Al}). g_0 is the free energy (per atom) of defect-free NiAl. Note that only three of the defect complexes are independent.

Defect complex	Notation	Constitution	Relation
Triple Ni	TN	$2V_{\mathrm{Ni}}+\mathrm{Ni_{Al}}$	$g_{\mathrm{TN}}=g_{\mathrm{Ni_{Al}}}+2g_{V_{\mathrm{Ni}}}+2g_0$
Divacancy	Dv	$V_{\mathrm{Ni}}+V_{\mathrm{Al}}$	$g_{\mathrm{Dv}}=g_{V_{\mathrm{Ni}}}+2g_{V_{\mathrm{Al}}}+2g_0$
Exchange	Ex	$\mathrm{Al_{Ni}}+\mathrm{Ni_{Al}}$	$g_{\mathrm{Ex}}=g_{\mathrm{Ni_{Al}}}+g_{\mathrm{Al_{Ni}}}$
Triple Al	TA	$2V_{\mathrm{Al}}+\mathrm{Al_{Ni}}$	$g_{\mathrm{TA}}=g_{\mathrm{Al_{Ni}}}+2g_{V_{\mathrm{Al}}}+2g_0$
Interbranch Ni	IN	$2V_{\mathrm{Al}}-\mathrm{Ni_{Al}}$	$g_{\mathrm{IN}}=2g_{V_{\mathrm{Al}}}-g_{\mathrm{Ni_{Al}}}+2g_0$
Interbranch Al	IA	$\mathrm{Al_{Ni}}-2V_{\mathrm{Ni}}$	$g_{\mathrm{IA}}=g_{\mathrm{Al_{Ni}}}-2g_{V_{\mathrm{Ni}}}-2g_0$

defect, in particular, turns out to be the lowest-energy thermal excitation on the Al-rich side of NiAl.[5]

Table I details the relations between the free energies of complex defects, g_{cd}, and the raw free energies of individual point defects, g_P. Similar expressions apply to cd potential energies u_{cd}, vibrational energies ε_{cd}^{vib}, and vibrational entropies s_{cd}^{vib}.

III. CALCULATION DETAILS

The QHA calculations were performed on a $8\times8\times8$ periodic supercell (1024 atomic sites) with or without a single point defect. At this supercell size defect formation energies and entropies converge to within 0.1%.[25] A static relaxation of the block was performed by the conjugate gradient algorithm until forces converged to better than 10^{-5} eV/Å and the relative change in the size of the supercell was smaller than 10^{-6}. Interactions between atoms were modeled with an EAM potential.[18]

The thermal expansion of defect-free NiAl was calculated within the QHA as described in Sec. II A. For QHA calculations of a defected block, the latter was first relaxed statically at $T=0$ K and then stretched uniformly by the thermal-expansion factor of the perfect lattice at a desired temperature.[26] This procedure assumes a negligible dependence of thermal expansion on the concentration of point defects. The validity of this assumption for NiAl is supported by the experimentally observed weak dependence of thermal expansion on the composition.[27] This assumption was also checked in the present study by MC simulations (see Sec. V B below).

The MC simulations were performed at a constant temperature, zero pressure, and a constant total number of lattice sites. A $10\times10\times10$ (2000 sites) periodic supercell was used in the simulations. Each MC run initially allowed the system to equilibrate for 5000 steps after which the statistics was collected during another 50 000 steps (an MC step includes N trial moves, where N is the number of atoms in a supercell). Two thermodynamic ensembles were simulated. In the canonical ensemble, a trial move consisted in an arbitrarily small displacement of a randomly chosen atom in a random direction. A maximum displacement was 0.1 Å along each Cartesian axis. After every 2000 trial moves of this type, a global move was attempted by scaling the size of the block by a random amount (maximum 0.1%). In the grand canonical ensemble, each trial displacement of an atom was accompanied by switching its chemical sort to a new one chosen at random between Ni and Al. In this ensemble, it is the difference between the chemical potentials of Ni and Al that is fixed, whereas the amounts of Ni and Al atoms can vary.

IV. RESULTS

Table II summarizes the calculated thermodynamic properties of the perfect lattice of NiAl. The numbers obtained by invoking the classical approximation and neglecting thermal expansion (first row of the table) are identical to those of Ref. 18. The difference between the free energies g_0 given in the first two rows represents the effect of zero-point vibrations, which includes the potential-energy change due to the lattice expansion as well as the energy of the zero-point motion itself. The latter contribution is seen to be dominant.

The calculated point defect characteristics in NiAl are summarized in Table III in the form of complex-defect properties. Zero-temperature potential energies of defect com-

TABLE II. Potential energy u_0, vibrational energy ε_0^{vib}, vibrational entropy s_0^{vib}, and free energy g_0 of stoichiometric NiAl (per atom) calculated within the QHA. The first row contains the results calculated within the classical approximation by neglecting thermal expansion (Ref. 18).

T(K)	u_0 (eV)	ε_0^{vib} (eV)	s_0^{vib}/k_B	g_0 (eV)
0	−4.47	0	6.31	−4.47
0	−4.46	0.047	0.00	−4.42
50	−4.46	0.048	0.17	−4.42
100	−4.46	0.052	0.74	−4.42
200	−4.46	0.067	1.99	−4.43
300	−4.46	0.088	3.00	−4.45
400	−4.46	0.111	3.80	−4.48
500	−4.46	0.136	4.46	−4.52
800	−4.46	0.211	5.90	−4.65
1000	−4.45	0.261	6.61	−4.76
1300	−4.44	0.338	7.50	−4.94
1500	−4.43	0.389	8.01	−5.08
1700	−4.42	0.441	8.49	−5.22

[a]Classical approximation.

TABLE III. Same as Table II but for composition-conserving defect complexes: triple-Ni defect (TN), divacancy (Dv), exchange defect (Ex), and interbranch-Al defect (IA).

T(K)	Potential energy u_{cd} (eV)				Vibrational energy ε_{cd}^{vib} (eV)				Vibrational entropy s_{cd}^{vib}/k_B				Free energy g_{cd} (eV)			
	TN	Dv	Ex	IA	TN	Dv	Ex	IA	TN	Dv	Ex	IA	TN	Dv	Ex	IA
0	2.28	2.40	2.77	0.48	0	0	0	0	3.59	2.97	4.90	1.32	2.28	2.40	2.77	0.48
0	2.28	2.40	2.77	0.48	−0.049	−0.024	−0.048	0.001	0.00	0.00	0.00	0.00	2.23	2.37	2.72	0.48
50	2.28	2.40	2.77	0.48	−0.046	−0.021	−0.044	0.002	0.92	1.29	1.45	0.53	2.23	2.37	2.72	0.48
100	2.28	2.40	2.77	0.48	−0.039	−0.014	−0.033	0.006	1.93	2.26	3.15	1.22	2.23	2.36	2.71	0.48
200	2.28	2.40	2.77	0.48	−0.027	−0.008	−0.018	0.009	3.01	2.79	4.43	1.42	2.20	2.34	2.67	0.47
300	2.28	2.40	2.77	0.48	−0.019	−0.005	−0.012	0.007	3.40	2.93	4.79	1.38	2.18	2.32	2.63	0.46
400	2.28	2.40	2.77	0.48	−0.014	−0.004	−0.009	0.006	3.61	2.99	4.97	1.35	2.15	2.29	2.59	0.44
500	2.29	2.40	2.77	0.48	−0.012	−0.003	−0.007	0.005	3.76	3.03	5.09	1.34	2.11	2.27	2.54	0.43
800	2.29	2.40	2.78	0.49	−0.007	−0.002	−0.004	0.003	4.00	3.04	5.42	1.42	2.01	2.19	2.40	0.39
1000	2.30	2.40	2.78	0.49	−0.005	−0.001	−0.003	0.002	4.09	3.00	5.63	1.54	1.94	2.14	2.29	0.36
1300	2.31	2.41	2.80	0.49	−0.004	−0.001	−0.003	0.001	4.19	2.85	6.06	1.88	1.83	2.09	2.11	0.28
1500	2.31	2.41	2.80	0.49	−0.003	−0.001	−0.002	0.001	4.28	2.76	6.44	2.16	1.76	2.06	1.97	0.21
1700	2.32	2.42	2.82	0.49	−0.003	0.000	−0.002	0.001	4.35	2.59	6.93	2.58	1.68	2.04	1.80	0.12

[a]Classical approximation.

plexes, u_{cd}, agree reasonably well with previous *ab initio* calculations (see, e.g., Table IX in Ref. 18 or Fig. 1 in Ref. 19). As in Table II, a comparison of the free energies g_{cd}, given in the first two rows of the table, reveals the effect of zero-point vibrations. The latter decreases the free energy of the TN and Ex complexes by about 0.05 eV and the free energy of a divacancy by about 0.025 eV. The free energy of the IA defect remains almost unaffected as a result of the cancellation of different contributions (notice that the IA, TN, and Ex complexes are linearly dependent: TN+IA =Ex).

The variation of the potential energy of the defect complexes with temperature is due to thermal expansion, whereas the changes in their vibrational energy is due to quantum effects. At high temperatures, ε_{cd}^{vib} tends to zero due to the equipartition theorem and cancellation of terms within a cd. The entropy of defect complexes depends on temperature significantly due to quantum effects at low temperatures and thermal expansion at high temperatures. The two effects account for the difference between the entropies calculated in the quantum and classical limits (note that the classical-limit entropy depends on the temperature implicitly through the volume-dependent vibrational frequencies and at high temperatures coincides with the quantum one, as it should).

The temperature dependence of the free energies of cd's is dominated by the $-Ts_{cd}^{vib}$ term, temperature variations of the complex energies being much weaker. To illustrate this fact, we plot in Fig. 1 the temperature dependence of the TN complex free energy relative to its value at $T=0$, $\Delta g_{TN}(T) = g_{TN}(T) - g_{TN}(0)$, together with individual contributions to this quantity. We clearly see that the entropy term $-Ts_{cd}^{vib}$ dominates. A similar behavior is observed for other cd's.

Surprisingly as it seems, we have not found in the literature any calculation of defect formation free energies and entropies in NiAl. However, some estimations do exist. Meyer and Fähnle[4] suggested that the vibrational entropy of the TN defect as large as $2.25k_B$ would be sufficient for bringing the results of their static calculations to agreement with thermodynamic activity measurements.[28,29] This entropy is in a reasonable agreement with our result ($4.19k_B$ at 1300 K), given the uncertainties involved in this comparison. Another estimation is given in Ref. 30, according to which the vibrational entropy of the TN defect at 1400 K is $7.5k_B$, which is again in a qualitative agreement with our entropy. However, the vibrational entropy of the Ex defect is assumed to be close to 0 (see Ref. 31 for details). Correspondingly, the IA entropy should be large and negative, i.e., $-7.5k_B$. Our

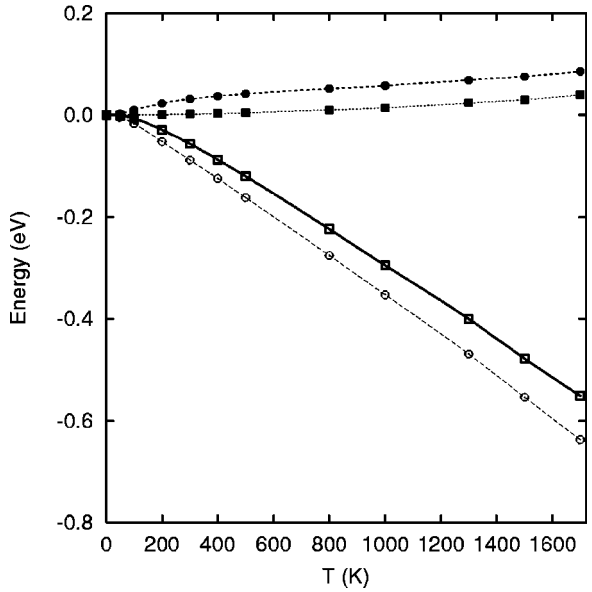

FIG. 1. Temperature dependence of the free energy of the triple-Ni defect complex relative to its value at 0 K, $\Delta g_{\mathrm{TN}} = \Delta u_{\mathrm{TN}} + \Delta \varepsilon_{\mathrm{TN}}^{vib} - Ts_{\mathrm{TN}}^{vib}$ (□). Δu_{TN}: potential energy (■); $\Delta u_{\mathrm{TN}} + \Delta \varepsilon_{\mathrm{TN}}^{vib}$: potential and vibrational energies (●); $-Ts_{\mathrm{TN}}^{vib}$: entropy contribution (○). The plot demonstrates the predominance of the Ts^{vib} term.

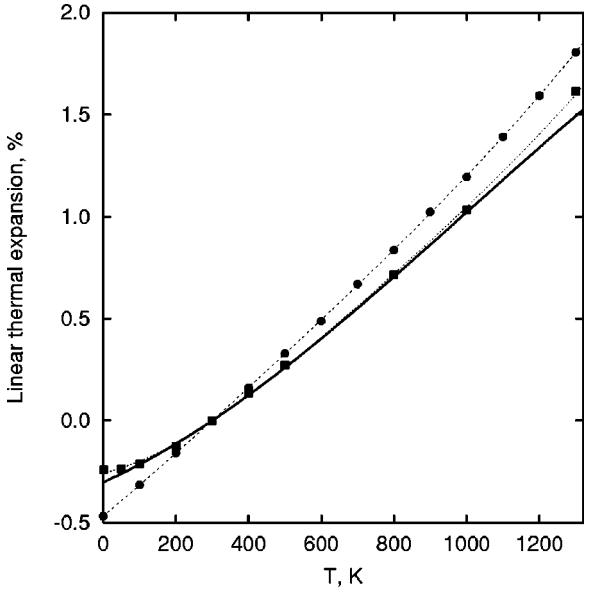

FIG. 2. Linear thermal expansion (relative to room temperature) of the perfect lattice of NiAl obtained by Monte Carlo simulations (●) and within the QHA (■) in comparison with experimental data (Ref. 35) (solid line).

results, on the contrary, demonstrate that the formation entropy of the exchange defect is positive and exceeds that of the triple-Ni defect in the whole temperature range (Table III). This makes s_{IA}^{vib} small and positive.

V. DISCUSSION

A. Thermal properties of defect-free NiAl

The effect of zero-point motion on lattice properties of NiAl is small but noticeable. The lattice parameter a_0 expands by 0.0081 Å, from 2.8587 Å to 2.8668 Å (the experimental value is 2.8870 Å[32]). The cohesive energy increases by 0.42 meV/atom. For comparison, zero-point vibrations were predicted[33] to change the lattice constant of Al from 3.98 Å to 4.00 Å ($a_0=4.05$ Å in experiment[34]).

Figure 2 demonstrates an excellent agreement between the calculated and experimental[35] values of the lattice expansion factor, which is understandable since thermal expansion was included in the fitting database of the EAM potential.[18] The MC calculations, which were performed in the canonical mode, are seen to slightly overestimate the expansion in comparison with QHA and experiment. The discrepancy begins to develop above 500 K, but the agreement with experiment is still quite good. At low temperatures the MC data are incorrect as they neglect quantum effects. As a result, the MC lattice parameter tends to its static value in the zero-temperature limit. The difference between the QHA and MC lattice constants extrapolated to $T=0$ K thus represents the effect of zero-point motion.

As another test of the QHA, we compare in Fig. 3 the temperature dependencies of the enthalpy h_0 and entropy s_0 of NiAl with recent experimental measurements[36] of the heat capacity C_p by taking advantage of the thermodynamic relations

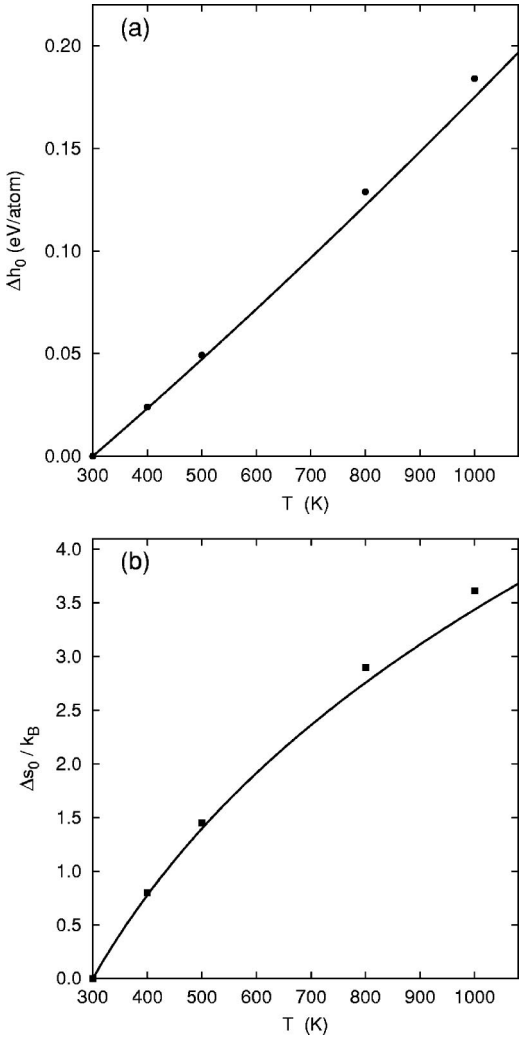

FIG. 3. Temperature dependence of thermodynamic functions of stoichiometric NiAl relative to 300 K. (a) Relative enthalpy $\Delta h_0(T)$ (●); (b) relative entropy $\Delta s_0(T)$ (■). Solid lines have been recalculated from the experimental C_p data for the 50.02 at % Al alloy reported in Ref. 36.

$$\Delta h_0(T) \equiv h_0(T) - h_0(T_0) = \int_{T_0}^{T} C_p(\tau)\, d\tau,$$

$$\Delta s_0(T) \equiv s_0(T) - s_0(T_0) = \int_{T_0}^{T} \frac{C_p(\tau)}{\tau}\, d\tau,$$

where $T_0=300$ K. These quantities are compared with QHA calculations, in which $h_0(T)=u_0(T)+\varepsilon_0^{vib}(T)$ (since $p=0$, the enthalpy is identical to energy) and $s_0(T)=s_0^{vib}(T)$ (Fig. 3). The agreement is rather encouraging, especially at low temperatures.

The constant-volume heat capacity C_V can also be obtained in the QHA by differentiating E^{vib} [see Eq. (4)] with respect to temperature at a constant volume:

$$C_V = k_B \sum_{\alpha=1}^{3n-3} \left(\frac{h\nu_\alpha}{k_B T}\right)^2 \frac{\exp(-h\nu_\alpha/k_B T)}{[1-\exp(-h\nu_\alpha/k_B T)]^2}.$$

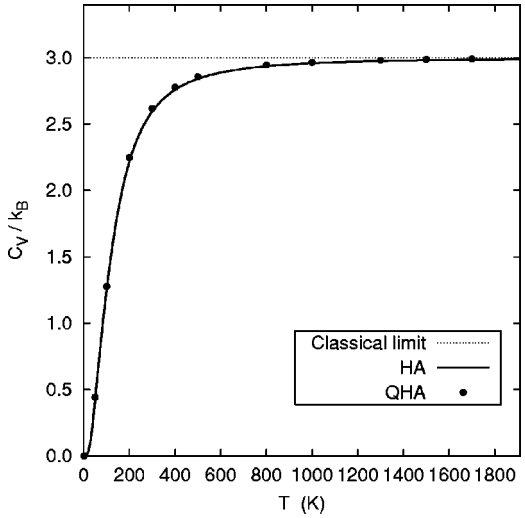

FIG. 4. Constant-volume heat capacity C_V of defect-free NiAl calculated within the QHA and HA. Both QHA and HA values tend to the classical limit at high temperatures.

The results of the calculation are shown in Fig. 4. They agree with the HA data (no thermal expansion) so well that the difference between the two sets of results is hardly seen in the plot.

This difference is more apparent, however, for a related quantity, namely, the Debye temperature $\Theta_D(T)$. In Fig. 5 we plot the high-temperature limit of the Debye temperature, Θ_D^∞, which describes the leading $(1/T^2)$ term in C_V as it approaches the Dulong-Petit value of $3k_B$ at high temperatures. Θ_D^∞ is defined[37] as

$$\Theta_D^\infty = k_B \sqrt{\frac{5}{3} h^2 \langle \nu^2 \rangle},$$

where $\langle \nu^2 \rangle$ is the mean-squared phonon frequency. By this definition, Θ_D^∞ does not depend on the temperature explicitly, hence the variation of Θ_D^∞ in Fig. 5 is solely due to thermal

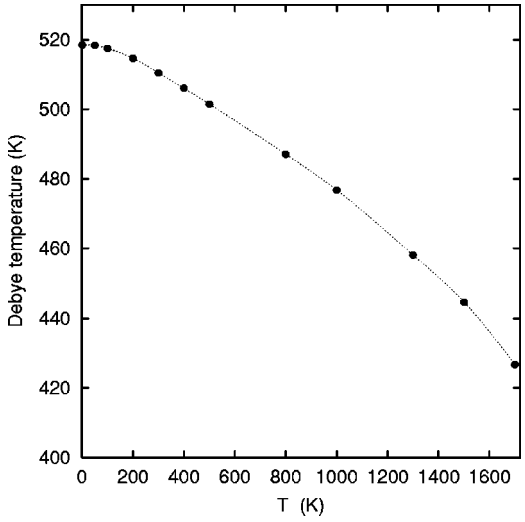

FIG. 5. Debye temperature of stoichiometric NiAl calculated within the QHA.

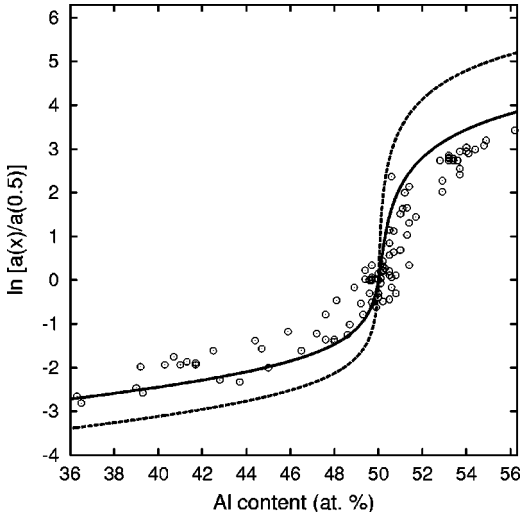

FIG. 6. Al activity in NiAl relative to the stoichiometric composition at 1237 K calculated within the QHA (solid line) and by static calculations neglecting atomic vibrations (dashed line). Experimental data (○) are from Ref. 28 [shifted by 1.5 at % Al (Ref. 29)].

expansion. The experimentally reported Debye temperature of nominally stoichiometric NiAl ranges from 470 K to 560 K.[38] In the context of our study, the significance of Debye temperature is twofold. First of all, it provides an estimate of the temperature above which all phonon states become populated. This means that below Debye temperature the classical consideration is likely to be inapplicable. On the other hand, Debye temperature is often used as an estimate for the temperature below which the underestimation of anharmonicity in the QHA is not important, even for systems with reduced symmetry (e.g., with defects). A more optimistic estimate of such temperature is $0.5T_m$,[17,26] where T_m is a melting point (1911 K for the stoichiometric NiAl).

Overall, the QHA combined with this EAM potential appears to provide a reasonable description of thermal properties of NiAl.

B. Chemical potentials

Steiner and Komarek[28] performed calorimetry measurement of Al activity in NiAl as a function of composition. The originally reported data were later recognized to contain a systematic error in alloy compositions,[27] hence in Fig. 6 they are shifted by 1.5 at % Al as recommended in Ref. 29. We compare these data with our QHA results as well as with calculations neglecting atomic vibrations. We see that atomic vibrations have a noticeable effect and improve the overall agreement with experiment. This improvement is mainly due to the vibrational entropy, whereas the effect of the temperature-dependent energy is negligible.

In Fig. 7 we compare the difference between the chemical potentials of Ni and Al, $\Delta\mu = \mu_{\mathrm{Ni}} - \mu_{\mathrm{Al}}$, obtained by QHA calculations and by MC simulations performed in the grand canonical mode. As the MC simulations do not allow for variations in the vacancy concentration, the vacancies were neglected and only Ni-rich compositions were calculated.

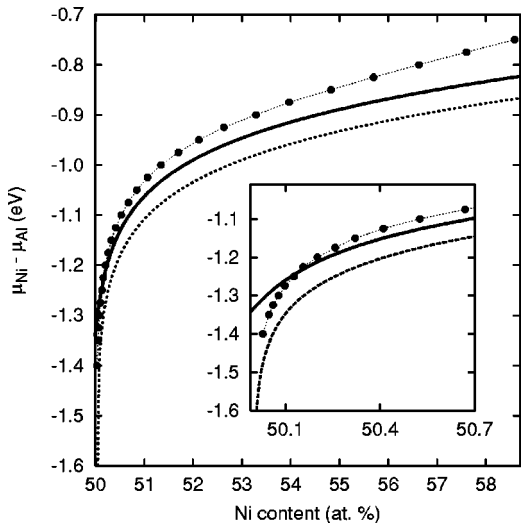

FIG. 7. The difference between the Ni and Al chemical potentials at 1200 K as a function of composition in Ni-rich NiAl calculated within the QHA (solid line) and by Monte Carlo simulations (●). The dashed line was calculated within the QHA by neglecting vacancies.

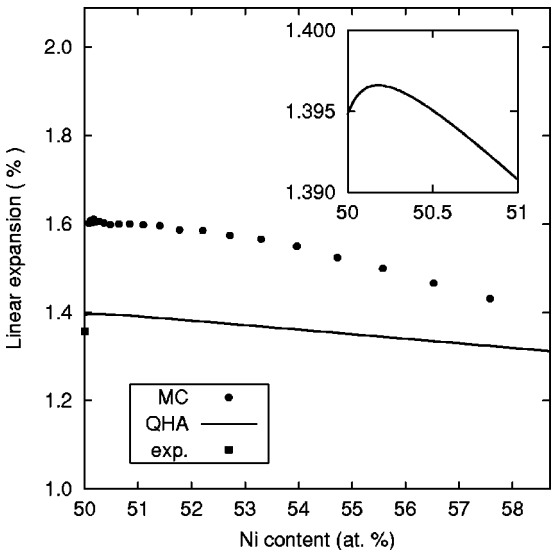

FIG. 8. Linear thermal expansion (relative to room temperature) at 1200 K as a function of composition in Ni-rich NiAl obtained by QHA and Monte Carlo calculations. The experimental point is from Ref. 35.

Both sets of results are in reasonable agreement with each other. A similar agreement was obtained in Ref. 22 using Finnis-Sinclair potentials.

The discrepancy between the QHA and MC data can be due to three factors: the different treatment of the lattice anharmonicity, defect-defect interactions, or the neglect of vacancies in the MC simulations. It is not possible to distinguish between the former two factors, but it is straightforward to check the latter. To do so, we have also calculated $\Delta\mu$ within the QHA by including antisites only, which was expected to make the QHA and MC calculations more consistent with each other. Surprisingly, this resulted in increasing the discrepancy between them in largely off-stoichiometric compositions. However, in the vicinity of the stoichiometric composition the MC curve correctly approaches the relevant QHA curve (see inset in Fig. 7). We can conclude that the neglect of vacancies in not the leading factor.

A distinction between the anharmonic effects and defect-defect interactions seems however possible in Fig. 8, in which the linear expansion factor of NiAl at the temperature of 1200 K relative to the perfect lattice at 300 K is shown as a function of composition. The data were obtained by QHA and MC calculations and, in contrast to Fig. 2, include the effect of point defects on the lattice parameter. The shift between the QHA and MC results around the stoichiometry mainly reflects the difference in the thermal expansion coefficients of the perfect lattice predicted by the two calculation methods (cf. Fig. 2). An interesting effect to notice in this plot is that the QHA and MC curves remain parallel to each other until almost 52 at % Ni, with relatively small deviations thereafter. This observation suggests that the variation of the lattice parameter with composition is rather insensitive to the concentration of thermal defects and is mainly due to the structural Ni_{Al} defects. It also provides another demonstration that the QHA is a reasonable approximation for point defects. The nonlinear behavior at higher Ni concentrations is likely due to the increased interactions between Ni_{Al} antisites. The downward turn of the linear-expansion coefficient in concentrated alloys suggests that these interactions are repulsive at short distances. Indeed, as the lattice expands the average distances between the vibrating Ni_{Al} defects increases, allowing the lattice parameter to slightly shrink. Such conclusion agrees with results of direct *ab initio*[5] and EAM[39,40] static calculations.

Another interesting feature revealed by Fig. 8 is the slight deviation of the QHA curve from a straight line near the stoichiometric composition (see in the inset). This effect is primarily caused by the TN defect whose effective formation free energy rapidly decreases near the equiatomic composition.[5] Both constituents of the TN defect, V_{Ni} and Ni_{Al}, reduce the average lattice parameter of the crystal, hence the QHA curve shows a downward turn. This effect offsets the maximum of the lattice constant away from the exact stoichiometric composition and is revealed not only in the QHA but also in static calculations neglecting atomic vibrations. In practice, this offset can be difficult to observe experimentally due to the limited accuracy of the chemical characterization of samples and possible local fluctuations of the composition.

C. Point defects in NiAl

1. Structural defects and zero-point vibrations

Since the question of whether V_{Ni} is indeed the structural defect in Al-rich NiAl has been the subject of recent debate in the literature, we will first check how zero-point vibrations can affect point defect energies. Indeed, although V_{Ni} is predicted to be the structural defect by all *ab initio* calculations,

a theoretical possibility exists that zero-point vibrations, unaccounted in those calculations, could revert the balance in favor of Al_{Ni} antisites.

In the absence of atomic vibrations, the energies of the IA and IN complexes predicted by the present EAM potential are positive: 0.484 eV and 2.511 eV, respectively (Table III). Hence, V_{Ni} and Ni_{Al} should be the structural defects. After including both the thermal expansion and the energy associated with zero-point motion, the free energies of the IA and IN complexes become 0.485 eV and 2.511 eV, respectively, i.e., change by less than 2 meV. This is not an amount of energy that could revert the sign of the IA and IN energies, which are 2–3 orders of magnitude larger. We, thus, conclude that zero-point vibrations do not alter the type of constitutional defects in NiAl.

2. Thermal defects

There are two basic questions regarding the effect of atomic vibrations on the statistics of point defects in NiAl: (1) How do the vibrations change the defect concentrations? and (2) do the vibrations change the dominant thermal excitation(s)?

In Fig. 9 we compare the concentrations of three independent defect complexes calculated with and without the vibrational contribution in the form of Arrhenius plots. The concentrations are shown for three different compositions: stoichiometric, slightly Ni rich, and slightly Al rich. The cd concentrations were obtained by combining individual point defect concentrations delivered by the statistical model (Sec. II B). The point defect behavior is fully characterized by any three independent cd's. It is convenient to choose the set {TN, Dv, Ex} for the stoichiometric and Ni-rich compositions and {TN, IA, TA} for the Al-rich composition. We clearly observe that atomic vibrations increase the concentrations of complex defects by shifting them up nearly uniformly on the logarithmic scale. This increase is consistent with the decrease of the respective complex free energies g_{cd} with temperature (Table III). The decrease in g_{cd}'s is largely due to the positive vibrational entropies s_{cd}^{vib} (Sec. IV). The fact that the atomic vibrations leave the slope of the $\ln c_{cd}(1/T)$ curves almost unaffected until rather high temperatures is explained by the relatively weak temperature dependence of the cd energies, $\varepsilon_{cd}=u_{cd}+\varepsilon_{cd}^{vib}$. Regarding the concentrations of individual point defects, they also increase due to atomic vibrations, except for the concentration of V_{Ni} vacancies in Al-rich NiAl (Sec. V C 3).

Regarding the second question, Fig. 9 shows that the TN complex still dominates in the stoichiometric and Ni-rich compositions. This means that V_{Ni} and Ni_{Al} remain the dominant thermal defects at all temperatures. The situation is different in Al-rich compositions, where either the IA or the TN complex prevails, depending on temperature. The effect of atomic vibrations is to shift the crossover point towards lower temperatures (Sec. V C 3). There is also a shift of the intersection point of the more energetic excitations, Dv and Ex, but this effect does not essentially change the point defect behavior in NiAl since these defect complexes do not share any individual point defect. In addition, their concentrations are too small to be of significance to NiAl properties.

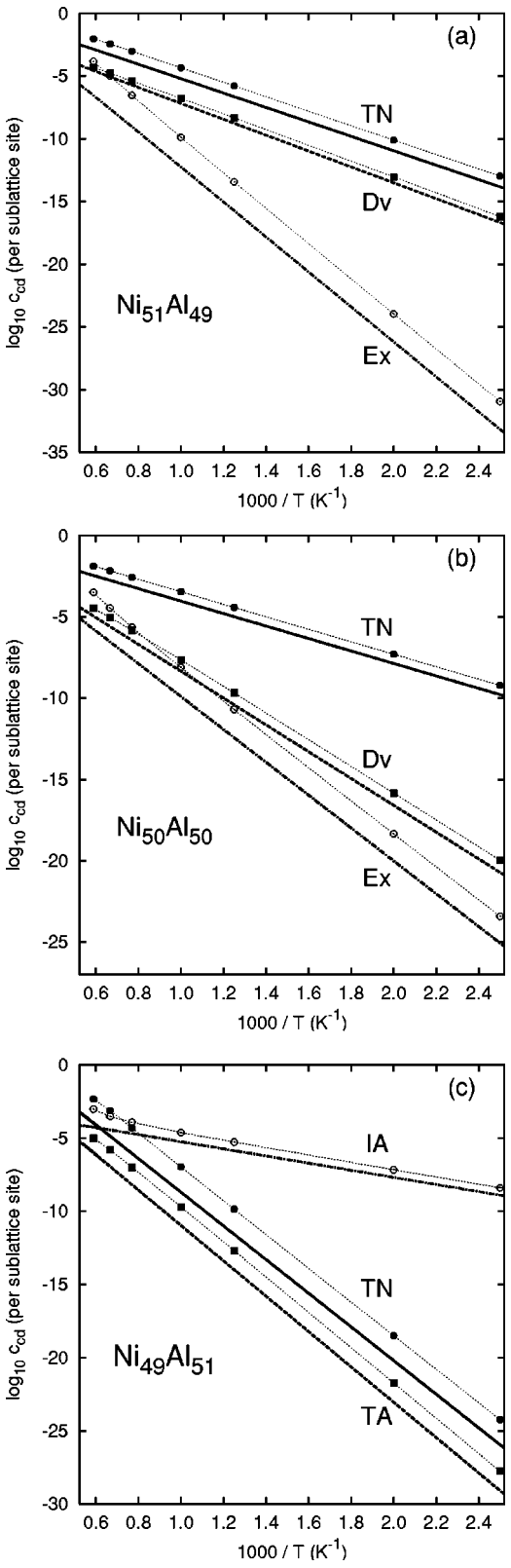

FIG. 9. Arrhenius plots of complex defect concentrations at three different compositions of NiAl. The points represent QHA results, and the lines were obtained by neglecting atomic vibrations. The left boundary of the plots corresponds to the melting temperature of stoichiometric NiAl (1911 K).

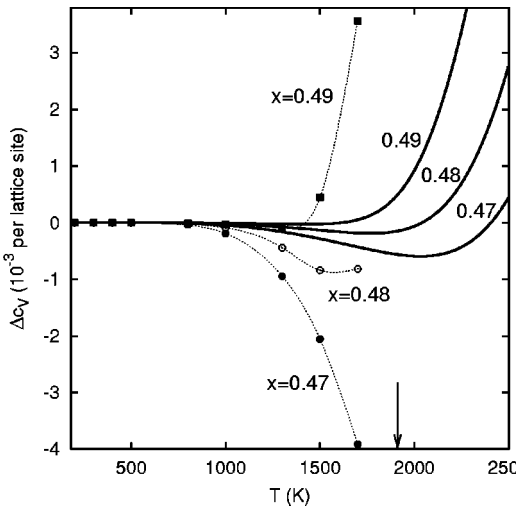

FIG. 10. Concentration of thermal vacancies $\Delta c_V(T) = c_V(T) - c_V(0)$ in Al-rich Ni_xAl_{1-x} ($x = 0.47$, 0.48, and 0.49) calculated within the QHA (points) and by neglecting atomic vibrations (solid lines). The vertical arrow marks the melting temperature of stoichiometric NiAl.

3. Vacancy concentration in Al-rich NiAl

Returning to Fig. 9(c), we observe a competition between the IN and TN complex defects at high temperatures. At small and medium temperatures, the IA complex strongly dominates, whereas near the melting point the TN complex takes over. This behavior, also noticed in previous *ab initio* calculations,[5,30,41] results in a minimum on the vacancy concentration versus temperature curve, $c_V(T)$. Indeed, each IA complex destroys two existing Ni vacancies, whereas each TN complex creates two new ones. Therefore, $c_V(T)$ should decrease with temperature if the IA complex dominates and increase if TN dominates. At the crossover point between the TN and IA branches, the concentration of Ni vacancies coincides with that at $T = 0$, therefore a minimum should occur at a slightly lower temperature.

To examine how the vibrations affect the position and depth of the minimum, we compare in Fig. 10 the thermal vacancy concentrations for three Al-rich compositions calculated within the QHA and using static point-defect energies. We see that the effect of atomic vibrations is to lower the temperature T_{min} of the minimum and to make the minimum deeper. The decrease in T_{min} is related to the larger vibrational entropy of the TN complex in comparison with IA, whereas the increase in the minimum depth is a more delicate effect involving an interplay between this entropy difference and the TN and IA free energies. The decrease in T_{min} agrees with the trend predicted by Meyer and Fähnle[30] on the basis of simple entropy estimates, but it is too small to account for the increase in the vacancy concentration with temperature around 1300 K found experimentally in the $Ni_{47}Al_{53}$ alloy.[14]

Although the QHA is not expected to predict very accurate numbers in the high-temperature range around T_{min}, we can conclude that the *changes* in both T_{min} and the depth of the minimum, c_{min}, are significant. Therefore, the effect of atomic vibrations should be taken into account in any attempt to rationalize experimental observations similar to those of Ref. 14. A comparison with experiment would be very useful for the assessment of theoretical models due to the high sensitivity of T_{min} and c_{min} to point defect energies and entropies. However, this kind of comparison requires further experimental measurements of the vacancy concentration at high temperatures. Suggestions for such experiments already appear in literature.[15]

VI. CONCLUSION

We have performed QHA as well as MC calculations in order to examine the effect of lattice vibrations on the structural and thermal point defects in NiAl. The calculated thermodynamic functions of the perfect lattice are in reasonable agreement with available experimental data, at least up to 1000–1300 K. The effect of zero-point vibrations turns out to be too small to affect the type of structural defects (V_{Ni} on the Al-rich side and Ni_{Al} on the Ni-rich side). Lattice vibrations result in an almost uniform (on the logarithmic scale) increase of the concentrations of all point defects. This increase is mainly related to the contribution from the vibrational entropy. The vibrational terms do not cause any qualitative changes in the statistics of thermal defects in NiAl. In stoichiometric and Ni-rich NiAl, the dominant thermal excitation remains the triple-Ni defect, whereas in Al-rich alloys the interbranch-Al defect competes with the triple-Ni defect. The effect of lattice vibration on the Al-rich side is to shift the characteristic minimum on the vacancy concentration versus temperature to lower temperatures and to make it deeper.

ACKNOWLEDGMENTS

This work was supported by the U.S. Air Force Office of Scientific Research through Grant No. F49620-01-0025. We thank Michael Finnis for useful comments on harmonic calculations and for providing his computer code used in this work for calculating the chemical potentials and point defect concentrations. One of us (A.Y.L.) wishes to thank Ruth Lynden-Bell for a clarification of some thermodynamical issues and for helpful comments on practical aspects of atomistic simulations.

[1] *Intermetallic Compounds: Structural Applications*, edited by J.H. Westbrook and R.L. Fleischer (Wiley, New York, 2000), Vol. 4.
[2] A.J. Bradley and A. Taylor, Proc. R. Soc. London, Ser. A **159**, 56 (1937).
[3] C.L. Fu, Y.-Y. Ye, M.H. Yoo, and K.M. Ho, Phys. Rev. B **48**, 6712 (1993).
[4] B. Meyer and M. Fähnle, Phys. Rev. B **59**, 6072 (1999).
[5] P.A. Korzhavyi, A.V. Ruban, A.Y. Lozovoi, Yu.Kh. Vekilov, I.A.

Abrikosov, and B. Johansson, Phys. Rev. B **61**, 6003 (2000).
[6] A. Alavi, A.Y. Lozovoi, and M.W. Finnis, Phys. Rev. Lett. **83**, 979 (1999).
[7] X. Ren, K. Otsuka, and M. Kogachi, Scr. Mater. **41**, 907 (1999).
[8] X. Ren and K. Otsuka, Philos. Mag. A **80**, 467 (2000).
[9] B. Meyer, G. Bester, and M. Fähnle, Scr. Mater. **44**, 2485 (2001).
[10] J. Breuer, F. Sommer, and E.J. Mittemeijer, Philos. Mag. A **82**, 479 (2002).
[11] T. Haraguchi and M. Kogachi, Mater. Sci. Eng., A **329-331**, 402 (2002).
[12] E.-T. Henig and H.L. Lukas, Z. Metallkd. **66**, 98 (1975).
[13] B. Bai and G.S. Collins, in *High Temperature Ordered Intermetallic Alloys VIII*, edited by E.P. George, M. Yamaguchi, and M.J. Mills, Mater. Res. Soc. Symp. Proc. **552** (Materials Research Society, Pittsburgh, 1999), pp. KK8.7.1–6.
[14] H.-E. Schaefer, K. Frenner, and R. Würschrum, Phys. Rev. Lett. **82**, 948 (1999).
[15] K.F. McCarty, J.A. Nobel, and N.C. Bartelt, Nature (London) **412**, 622 (2001).
[16] A.A. Maradudin, E.W. Montroll, G.H. Weiss, and I.P. Ipatova, *Theory of Lattice Dynamics in the Harmonic Approximation*, 2nd ed. (Academic Press, New York, 1971).
[17] J.M. Rickman and R. LeSar, Annu. Rev. Mater. Res. **32**, 195 (2002).
[18] Y. Mishin, M.J. Mehl, and D.A. Papaconstantopoulos, Phys. Rev. B **65**, 224114 (2002).
[19] Y. Mishin, A.Y. Lozovoi, and A. Alavi, Phys. Rev. B **67**, 014201 (2003).
[20] M.W. Finnis, in *Properties of Complex Inorganic Solids*, edited by A. Gonis, A. Meike, and P.E.A. Turchi (Plenum Press, New York, 1997).
[21] Y. Mishin and D. Farkas, Philos. Mag. A **75**, 169 (1997).
[22] M. Hagen and M.W. Finnis, Philos. Mag. A **77**, 447 (1998).
[23] Y. Mishin and C. Herzig, Acta Mater. **48**, 589 (2000).
[24] C. Wagner and W. Schottky, Z. Physik. Chem. B **11**, 163 (1930).
[25] Y. Mishin, M.R. Sørensen, and A.F. Voter, Philos. Mag. A **81**, 2591 (2001).
[26] S.M. Foiles, Phys. Rev. B **49**, 14 930 (1994).
[27] R.D. Noebe, R.R. Bowman, and M.V. Nathal, Int. Mater. Rev. **38**, 193 (1993).
[28] A. Steiner and K.L. Komarek, Trans. Metall. Soc. AIME **230**, 786 (1964).
[29] R. Krachler, H. Ipser, and K.L. Komarek, J. Phys. Chem. Solids **50**, 1127 (1989).
[30] B. Meyer and M. Fähnle, Phys. Rev. B **60**, 717 (1999).
[31] M. Fähnle, G. Bester, and B. Meyer, Scr. Mater. **39**, 1071 (1998).
[32] A. Taylor and N.J. Doyle, J. Appl. Crystallogr. **5**, 201 (1972).
[33] A.A. Quong and A.Y. Liu, Phys. Rev. B **56**, 7767 (1997).
[34] C. Kittel, *Introduction to Solid State Physics* (Wiley-Interscience, New York, 1986).
[35] *Thermal Expansion. Metallic Elements and Alloys*, edited by Y.S. Touloukian, R.K. Kirby, R.E. Taylor, and P.D. Desai, Thermophysical Properties of Matter Vol. 12 (Plenum, New York, 1975).
[36] L. Perring, J.J. Kuntz, F. Bussy, and J.C. Gachon, Intermetallics **7**, 1235 (1999).
[37] D.C. Wallace, *Thermodynamics of Crystals* (Dover, Mineola, New York, 1998).
[38] D.B. Miracle, Acta Metall. Mater. **41**, 649 (1993).
[39] Y. Mishin and D. Farkas, Philos. Mag. A **75**, 187 (1997).
[40] P. Gumbsch (private communication).
[41] P.A. Korzhavyi, I.A. Abrikosov, and B. Johansson, in *High Temperature Ordered Intermetallic Alloys VIII*, edited by E.P. George, M. Yamaguchi, and M.J. Mills, Mater. Res. Soc. Symp. Proc. **552** (Materials Research Society, Pittsburgh, 1999), pp. KK5.35.1–8.